JOURNAL OF MATERIALS SCIENCE 24 (1989) 2401–2407

Imperfections and impurity phases in flux grown $RCrO_3$ (R = La, Yb) single crystals

P. N. KOTRU, ASHOK K. ŘAZDAN
Department of Physics, University of Jammu, Jammu Tawi-180 001, India
B. M. WANKLYN
Department of Physics, Clarendon Laboratory, University of Oxford, Oxford, UK

Results of scanning electron microscopy (SEM) and energy dispersive X-ray analytical (EDAX) investigations, conducted on some elevated structures displayed by flux grown rare earth orthochromite, $RCrO_3$ (R = La, Yb) crystals, are presented. The peculiar structures exhibited by crystal surfaces indicate imperfections and impurity phases. EDAX of elevated structures reveals the various phases to be composed of lead associated materials which may probably be either Pb_2CrO_5 or Pb_2OF_2 (flux). Other secondary crystallization of impurity phases, ROF (R = La, Yb) is illustrated in the case of $RCrO_3$ (R = La, Yb) crystals. The elevated structures illustrate their non-stoichiometric behaviour. Precipitation of impurity phases and formation of imperfections during the growth of $RCrO_3$ (R = La, Yb) crystals and their effect on the crystalline quality is discussed.

1. Introduction

The rare earth orthochromites have a structure which is only slightly distorted from that of the perfect cubic perovskite. Its high degree of symmetry and the interaction between the Cr^{3+} and rare-earth ion make the compound suitable for investigation of its optical and magnetic properties. Attempts to grow crystals of $RCrO_3$ were made by Remeika [1] who reported the growth of small crystals from a Bi_2O_3 flux. Wanklyn [2] reported the growth of $RCrO_3$ crystals by isothermal evaporation using PbF_2–PbO–B_2O_3 flux. It is necessary that any growth technique yields crystals of very high purity and perfection. From this point of view the technique of growing the crystals can be perfected only if (1) the controlling factors of the impurities are known, and (2) the impurities which precipitate during the growth of a particular crystal, are identified.

Undesirable impurities have a detrimental effect on the physical and chemical perfection of a grown material; they may also influence the physical properties of the material. The scientific and technical application of the material will ultimately lie in how it is grown. The answer lies in understanding the growth process itself.

Flux growth has the advantage of producing crystals with habit faces as is the case with natural growth. Such crystals are best suited for surface structural studies which have provided significant information, as reported by Kotru *et al.* on flux grown crystals of rare earth orthoferrites [3–8] and $LaBO_3$ [9] crystals. The formation of secondary phases, their manifestation in different forms and their influence on the growth and development of $RFeO_3$ crystals is reported in [3–8]. Magnetoplumbite is the most frequently observed impurity phase in $RFeO_3$ crystal growth [5–8]. Crystallization of ROF (R = Dy, Ho, Er), RBO_3 (R = Dy, Er), $DyVO_4$, presence of aluminium (with $ErFeO_3$ and $HoFeO_3$) and silicon ($HoFeO_3$) as impurities in the flux growth of rare earth orthoferrites have been reported [5–8].

In order to understand the problem of precipitation of impurity phases for the growth of $RCrO_3$ crystals, scanning electron microscopic (SEM) and energy dispersive X-ray analytical (EDAX) studies were carried out on their surfaces. In this paper a report on the imperfections and formation of impurity phases as investigated through surface structural studies of rare earth orthochromites, $RCrO_3$ (R = La, Yb), is given. It may be noted that no data of this kind has been reported so far.

2. Experimental techniques

The crystals used here were grown by the flux technique using PbF_2–PbO–B_2O_3 [2]. The starting composition for $LaCrO_3$ consisting of 26.5 g La_2O_3, 12.4 g Cr_2O_3, 215 g PbF_2, 1 g PbO_2 and 6 g B_2O_3, was thoroughly mixed and pressed into a 100 cm^3 platinum crucible with a loosely-fitting lid and after holding at 1240° C for 10 days, was allowed to cool at 3–4° C h^{-1}. $YbCrO_3$ was prepared similarly using 32 g Yb_2O_3 and 12.3 g Cr_2O_3. The crystals were separated mechanically from the flux and then cleaned by heating in 20% nitric acid. The crystal surfaces were examined by SEM (Cambridge Stereoscan S4-10) and EDAX spectrometer (KeVx) attached to the scanning unit.

3. Results and discussion

A wide variety of surface structures has been displayed by the surfaces of single crystals of rare earth

0022–2461/89 $03.00 + .12

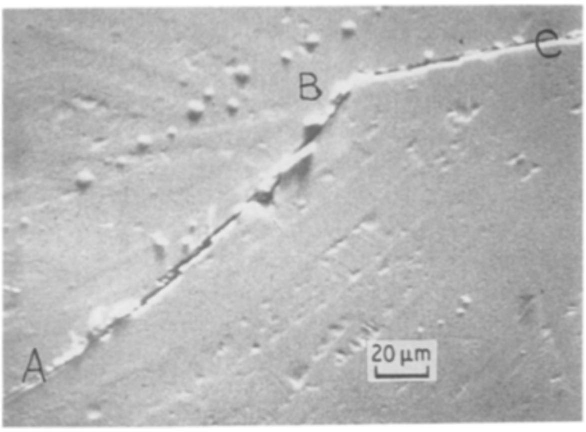

Figure 1 A scanning electron micrograph showing a crack A–B–C on the surface of a $LaCrO_3$ crystal.

orthochromites, $RCrO_3$ (R = La, Yb). However, there are a large number of samples which show imperfect faces and typical structures where the composing elements of $RCrO_3$ are not in a stoichiometric ratio. The description of these structures is mentioned in the subsequent sections.

3.1. Phases associated with lead

3.1.1. $LaCrO_3$ (*lanthanum orthochromite*)

Figure 1 is a scanning electron micrograph showing a crack A–B–C on the crystal surface of $LaCrO_3$. It is noticed from the micrograph that the crack might have accumulated some material at various places. A portion of the crack of the arm A–B of Fig. 1 is displayed, at a higher magnification, by Fig. 2a. The elemental line profile along the route A–B–C–D of Fig. 2a is recorded by EDAX spectrometer. Fig. 2b shows the profile thus obtained. From the Figs. 2a and b one can significantly note the following:

(1) The two regions A–B and C–D, which are the parts of plane surface of the crystal, show normal presence of the elements of $LaCrO_3$. The profiles of $LaL\alpha$ (A_2–B_2 and C_2–D_2) and $CrK\alpha$ + $LaL\beta_2$(A_1–B_1 and C_1–D_1) support the statement as shown in Fig. 2b.

(2) The profiles due to $LaL\alpha$ (B_2–C_2) and $CrK\alpha$ + $LaL\beta_2$(B_1–C_1) of Fig. 2b corresponding to the region B–C of Fig. 2a tend to fall down from the normal route. Their fall is almost observed in the first half of the region B–C. The behaviour of these profiles in the second half of the region B–C shows that the relative concentration of La and Cr is lesser than that of the region C–D.

(3) $PbM\alpha$ (B_3–C_3) has a noticeable rise in the middle portion of region B–C of Fig. 2a.

From the above observations it is obvious that within the cracked portion there is a material rich in lead at the cost of lanthanum and chromium. It, there-

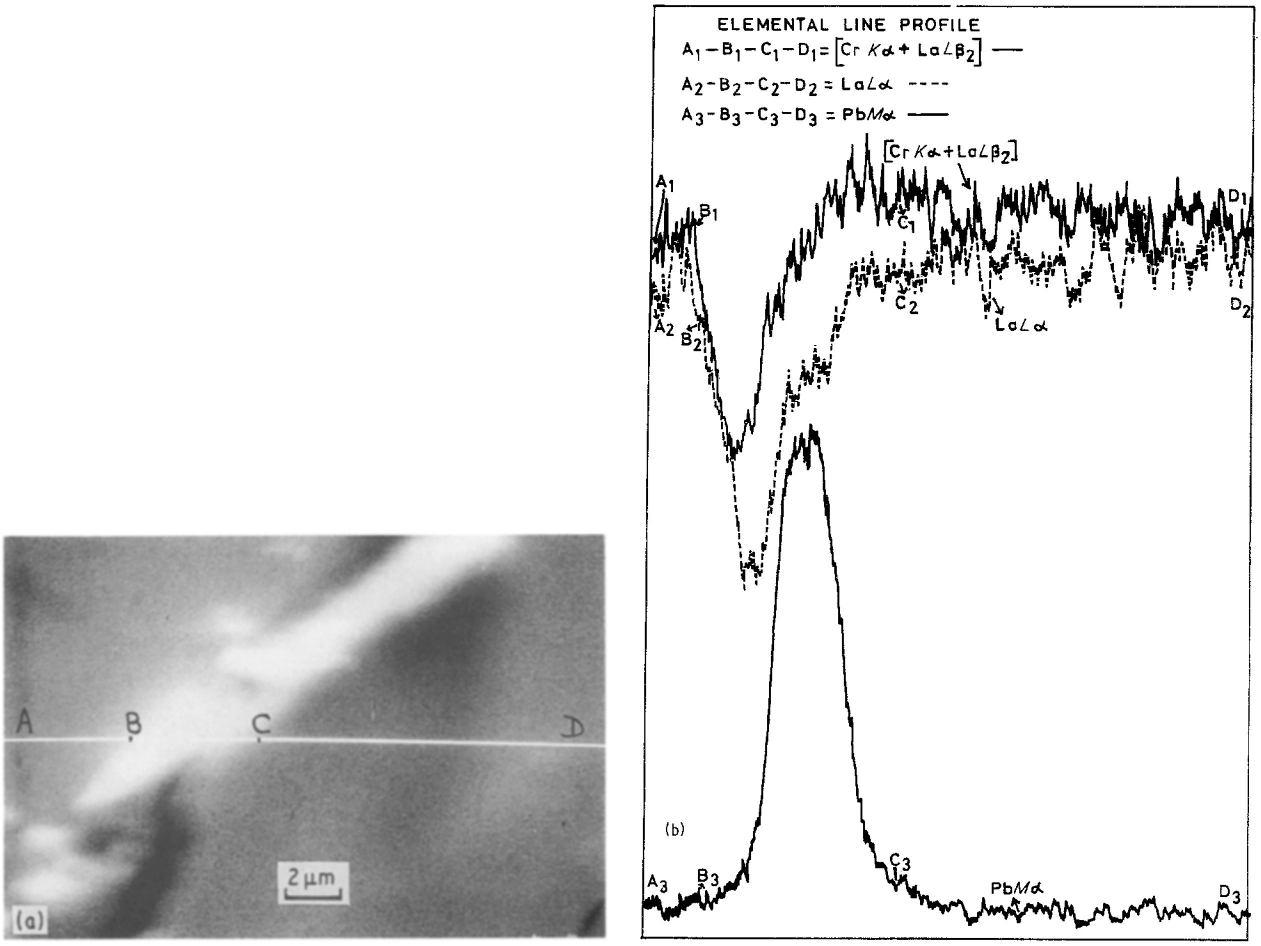

Figure 2 (a) SEM illustrating a portion of crack A–B of Fig. 1 at a higher magnification. The white line marked A–B–C–D is the route of line scan. (b) Line profile traced by EDAX spectrometer along the route A to D of Fig. 2a showing the distributions of the elements, Cr, La and Pb. The profile corresponding to $LaL\alpha$ has been reproduced in dotted shape for convenience to avoid confusion due to overlapping.

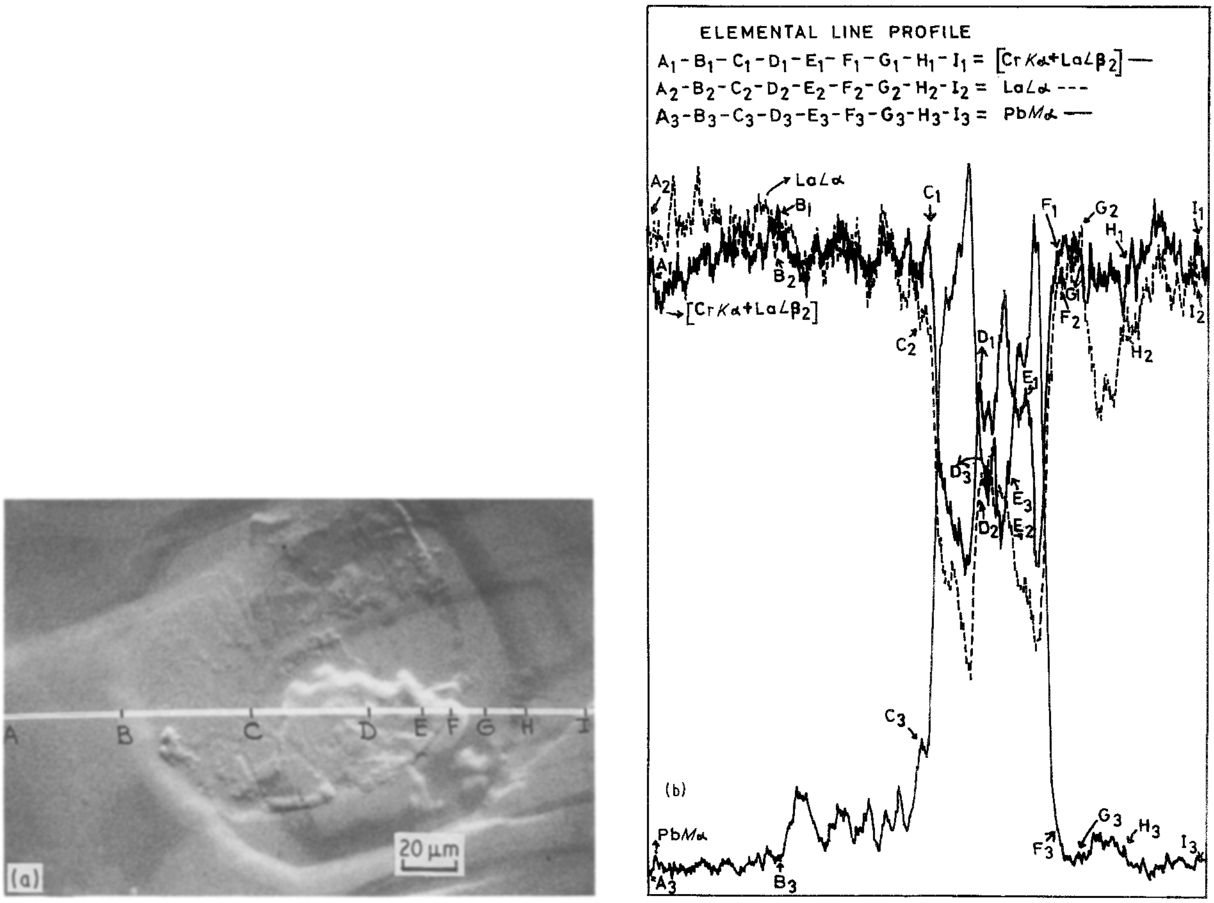

Figure 3 (a) SEM showing a circular elevated structure on the crystal surface of $LaCrO_3$. The line A–B–C–D–E–F–G–H–I is the track along which line scan has been traced by EDAX spectrometer. (b) Elemental line profile illustrating the distribution of elements La, Cr and Pb from A to I of Fig. 3a.

fore, seems that the crack becomes a preferential source for the trapping of material containing lead.

The surfaces of $LaCrO_3$ display some typical elevated structures where the composing elements are present in non-stoichiometric ratios. Fig. 3a is such an example showing an almost circular elevated structure recorded on the surface of $LaCrO_3$ crystal by SEM. One is able to notice the patch-like growth or depositions (C–F) within the periphery of an elevated structure. EDAX reveals a large deviation in the stoichiometry of this growth or deposition from a normal surface of the crystal. Fig. 3b is the elemental line profile recorded along the route A–B–C–D–E–F–G–H–I of Fig. 3a. The following points, on examining the Figs 3a and b, are interesting to note:

1. The region A–B (Fig. 3a), which is a part of the general surface shows normal presence of elements of $LaCrO_3$. The relative concentration of lanthanum and chromium is in stoichiometric order as evinced by A_2–B_2 and A_1–B_1 of Fig. 3b, respectively.
2. The region B–C (Fig. 3a) which forms a part of the elevated structure, shows the presence of Pb(B_3–C_3) in small traces besides the normal presence of La(B_2–C_2) and Cr(B_1–C_1).
3. There is a sudden decrease in relative concentration of La(C_2–D_2) and Cr(C_1–D_1) in the region C–D of Fig. 3a; the region forms a part of the patch-like deposition (C–F). The profile due to Pb(C_3–D_3) attains the maximum height indicating its presence at the cost of lanthanum and chromium.
4. In the region D–E of Fig. 3a, there is some recovery in the profiles corresponding to La(D_2–E_2) and Cr(D_1–E_1) as compared to the same profiles in the regions C_2–D_2 (La) and C_1–D_1 (Cr) of the Fig. 3b. The restoration of these profiles is not joining the original base line which shows the normal presence of the elements whereas the profile due to Pb(D_3–E_3) falls down but not to its base (zero) level, thereby showing its presence in very low concentrations. This clearly suggests that while the concentration of lanthanum and chromium starts rising, the concentration of lead falls.
5. The profiles in the region E–F of Fig. 3a, which is again a part of the patch-like deposition, repeat their behaviour in the same manner as does the region C–D. The profiles of La(E_2–F_2) and Cr(E_1–F_1) fall down whereas the profile due to Pb(E_3–F_3) rises up. This also supports the suggestion that the presence of lead occurs at the expense of lanthanum and chromium.
6. In the region F–G, the profiles of La(F_2–G_2) and Cr(F_1–G_1) get restored to their original base lines indicating their normal concentration whereas Pb(F_3–G_3) falls to zero level showing its absence.
7. In the region G–H, the profile due to La(G_2–H_2) falls down to some extent and profile of Cr(G_1–H_1) displays its normal presence. Further, the profile of Pb(G_3–H_3) shows a slight rise. The behaviour of profiles in this region suggests that lead is present at a lower concentration as compared to the normal concentration of chromium. But the concentration of lanthanum is decreased showing almost its absence. The presence of chromium and lead in this region

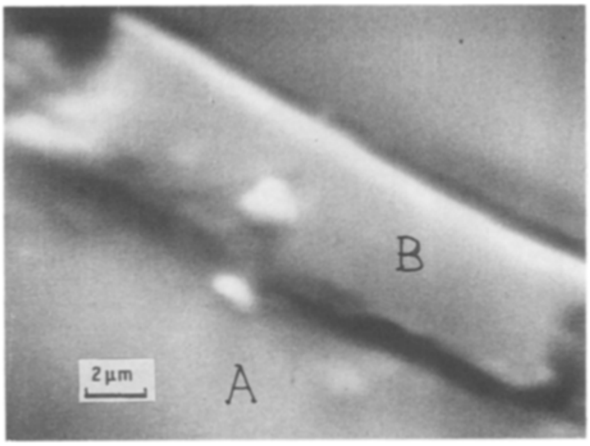

Figure 4 SEM of crystal surface of $YbCrO_3$ displaying a rectangular elevated structure B.

may suggest the crystallization of Pb_2CrO_5; but the resulting phase would be in non-stoichiometric proportions.

8. The profiles of La(H_2–I_2) and Cr(H_1–I_1) of the region H–I of Fig. 3a continue to show their normal presence as is the case with normal surface.

From the aforementioned observations, it follows that the deposition on the elevated structure mainly contains lead whose concentration increases at the expense of lanthanum and chromium, (C–D and E–F of Fig. 3a). But in the region B–C, lead is not present at the expense of lanthanum and chromium. The behaviour of profiles in the region G–H evidences the presence of lead and chromium.

Since the precipitation of metallic lead alone is ruled out as it dissolves in HNO_3 and the structure (Fig. 3a) was not washed off by the acid cleaning. The lead, however, is readily available from the flux (PbO–B_2O_3–PbF_2) used for the growth of crystals. The material containing lead is likely to be either flux combined with lanthanum orthochromite or lead combined with lanthanum, chromium and oxide (B–C, C–D, E–F of Fig. 3a and B–C of Fig. 2b). The precipitation of Pb_2CrO_5 may also be possible (G–H of Figs 3a and b) since this material has been prepared as single crystals from a melt containing Cr_2O_3, PbO and PbF_2 [10]. The elevated structure, therefore, is a region on the crystal surface where the elements of $LaCrO_3$ are not in stoichiometric proportions.

The precipitation of lead-containing materials has also been reported in case of $DyFeO_3$ [8] and $LaBO_3$ [9] crystals which were prepared from the flux systems PbO–PbF_2–B_2O_3 and PbO–B_2O_3, respectively. Also is reported the crystallization of magnetoplumbite ($PbFe_{12}O_4$) as a secondary phase in the case of $ErFeO_3$ [5], $HoFeO_3$ [7] and $DyFeO_3$ [8] crystals.

It may be noted that the detection of light elements, e.g. oxygen, fluorine and boron, was difficult by the EDAX technique used in the present investigation due to a number of reasons [11].

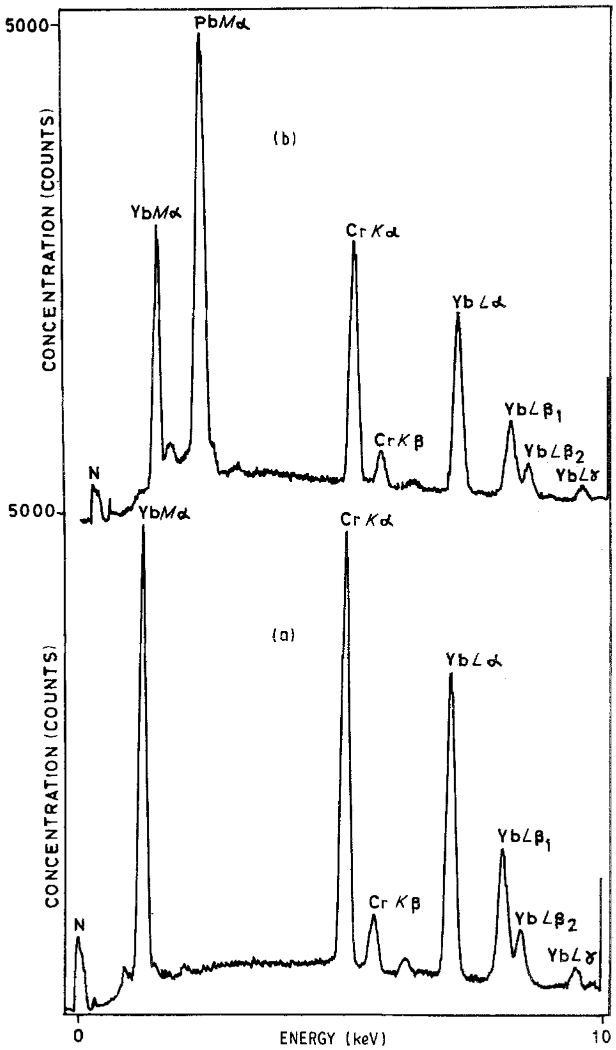

Figure 5 EDAX spectra recorded on (a) the general surface A away from the rectangular structure, (b) the rectangular structure B showing the presence of Pb$M\alpha$ peak in addition to the energy peaks due to ytterbium and chromium.

3.1.2. $YbCrO_3$ (ytterbium orthochromite)

The surface of the $YbCrO_3$ crystal also displays some structures whose chemical composition differs from that of general surface. Fig. 4, an electron micrograph, is one such example showing a nearly rectangular elevated structure marked as B. It appears the growth of the structure has taken place within the crack. EDAX was carried out on the general surface marked A and on the elevated structure B. Figs 5a and b are EDAX spectra recorded on the regions A and B of Fig. 4, respectively. From the investigation of EDAX spectra the following points emerge:

1. Fig. 5a shows the energy peaks due to ytterbium (Yb$M\alpha$, Yb$L\alpha$, Yb$L\beta_1$, Yb$L\beta_2$ and Yb$L\gamma$) and chromium (Cr$K\alpha$ and Cr$K\beta$). The analysis of the spectrum indicates that the region A is composed of ytterbium and chromium as expected for $YbCrO_3$.

2. Fig. 5b displays a peak due to lead (Pb$M\alpha$) besides the peaks due to ytterbium and chromium. It is inferred that the elevated structure B is composed of lead associated materials (either flux, Pb_2OF_2, combined with ytterbium orthochromite or lead combined with ytterbium, chromium and oxide).

Another type of elevated structure is shown by Fig. 6a whose shape is like a musical pipe of a snake charmer. The white line A–B–C–D is the route across the Fig. 6a along which the elemental line profile is recorded. The profile of elements is displayed by

Fig. 6b. It is evident from the profiles that there is a drop in the concentration of Yb(B_2–C_2) and Cr(B_1–C_1) to a minimum in the region B–C of Fig. 6a showing their absence. The profile due to lead (Pb$M\alpha$) is present in varying concentrations as shown by B_3–C_3 of Fig. 6b. But the relative concentration of Yb(A_2–B_2 and C_2–D_2) and Cr(A_1–B_1 and C_1–D_1) is normal in the regions A–B and C–D of Fig. 6a, respectively, as expected for $YbCrO_3$. It is clearly understood that the elevated structure (Fig. 6a) is composed of lead-containing material, which could be undissolved or incompletely dissolved flux (Pb_2OF_2); and the respective profiles of ytterbium and chromium evince almost their absence from the structure B–C of Fig. 6a.

As the typical structures associated with different impurity phases do not display any modification of growth fronts so their formation takes place evidently after the cessation of crystal growth.

3.2. *Formation of ROF (R = La, Yb) phases.*

3.2.1. $LaCrO_3$

The crystal surface of $LaCrO_3$ has exhibited a typical structure as shown by Fig. 7a. The structure appears to be an irregular elevation. The white line A–B–C–D across the elevation is the route along which elemental line scan is recorded. The profile of Fig. 7b reveals the fluctuations in the concentration of elements of crystal. On examining the Figs 7a and b, the following points are noteworthy:

1. Along A–B and C–D the elements of lanthanum and chromium of Fig. 7a show their normal presence as evidenced by the profiles of La(A_2–B_2 and C_2–D_2) and Cr(A_1–B_1 and C_1–D_1), of Fig. 7b.

2. There is an appreciable rise of profile due to La$L\alpha$(B_2–C_2) showing its presence whereas the profile corresponding to Cr$K\alpha$ + La$L\beta_2$ has a considerable fall (B_1–C_1) as is observed in the Fig. 7b. This indicates the absence of chromium in the region B–C of Fig. 7a. It may be noted here that the profile should have dropped to the minimum showing the absence of chromium. Since the profile corresponding to Cr$K\alpha$ + La$L\beta_2$ cannot be separated due to the resolution limitations of the instrument.

3. The profile corresponding to Pb$M\alpha$ shows a significant rise only at the edge B and a slight rise just at the edge C of the irregular elevation B–C of the Fig. 7a. It may be noted from the profile of Pb (A_3–B_3 and C_3–D_3) that lead is absent in the regions A–B and C–D of Fig. 7a.

From the above analyses it is inferred that the irregular structure is mainly composed of lanthanum associated with other elements. In order to further confirm the absence of any other possible elements, for example, lead and chromium, point EDAX was recorded in the middle portion of the structure B–C. Fig. 7c is the EDAX spectrum showing the peaks only due to lanthanum (La$L\alpha$, La$L\beta_1$, La$L\beta_2$ and La$L\gamma$). The peaks due to lead and chromium were noticed to be completely absent. The energy spectrum as displayed by Fig. 7c was also repeated over the whole region of elevated structure B–C to confirm the presence of lanthanum and the absence of chromium and lead.

The aforesaid analyses confirm that lanthanum is present as the main metallic component of the structure B–C. But it is not possible for lanthanum to be present as a metal because it is far too reactive. The elevated structure could be either the crystalline phase of LaOF or $LaBO_3$. Since the $LaCrO_3$ crystal had been

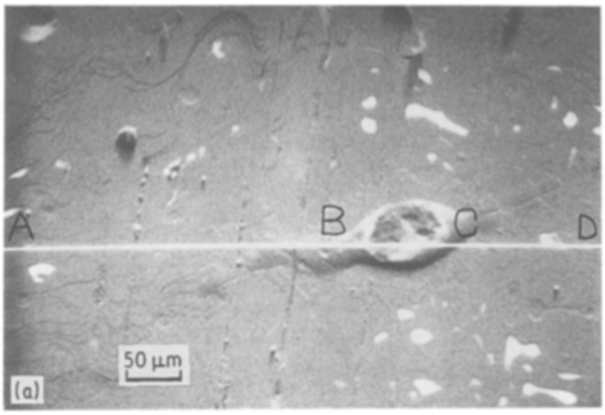

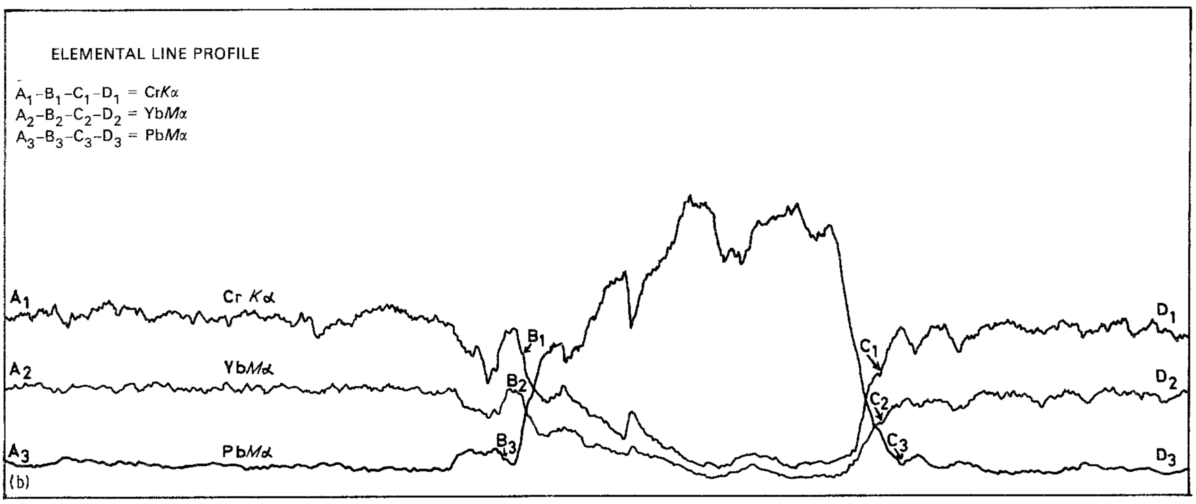

Figure 6 (a) SEM showing an elevated structure. The white line A–B–C–D is the route of the elemental scan. (b) Line profile traced in the region B–C of Fig. 6a showing the distribution of various elements.

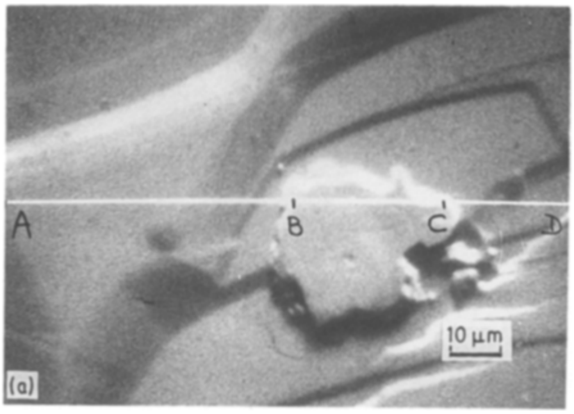

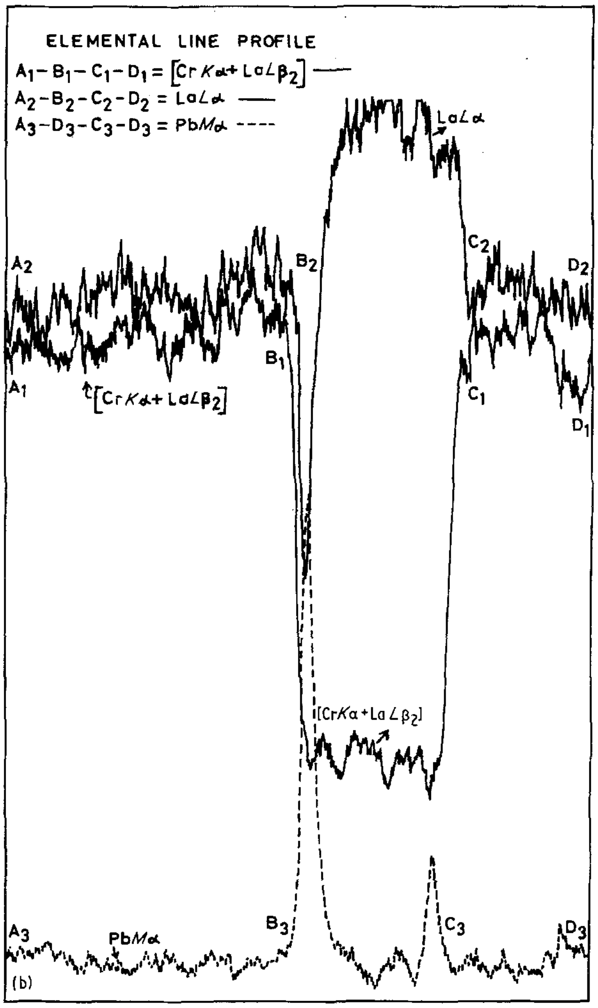

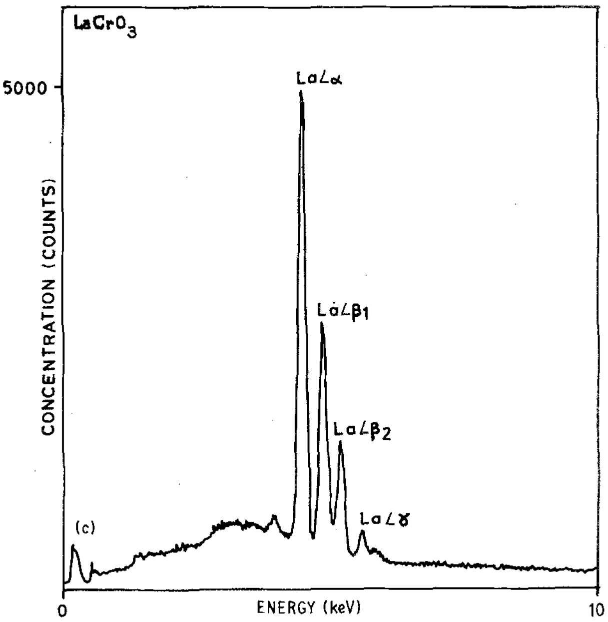

Figure 7 (a) SEM illustrating an irregular elevation on the $LaCrO_3$ crystal. A–B–C–D is the track along which elemental scanning was done. (b) Line profile detecting the distribution of La, Cr and Pb along the route A to D of Fig. 7a. (c) EDAX spectrum (point analysis) recorded in the middle portion of elevation B–C showing the presence of lanthanum only.

cleaned in nitric acid the crystallization of $LaBO_3$ is ruled out as it dissolves in the acid. Hence another possible phase is LaO_xF_{1-x}, which is generally called LaOF. It is more likely that the crystallization of impurity phase LaOF takes place on the crystal surface which results into the irregular structure shown here. The edges of structure B–C show only lead peaks which could be due to adhered materials containing lead (probably Pb_2OF_2).

3.2.2. $YbCrO_3$

Fig. 8a is a scanning electron micrograph displaying a triangular structure B–C on the surface of a $YbCrO_3$ crystal. EDAX studies indicate the feature to be associated with ytterbium and not with chromium. The elemental line scan recorded across A–B–C–D of Fig. 8a as displayed in Fig. 8b clearly reveals the following:

1. Along A–B and C–D both Yb(A_1–B_1 and C_1–D_1) and Cr(A_2–B_2 and C_2–D_2) are present as to be expected on a $YbCrO_3$ surface.
2. Along B–C there is a rise in the concentration of ytterbium and a drop in chromium concentration as evinced by B_1–C_1 and B_2–C_2 of Fig. 8b, respectively.

This suggests that the elevated feature is due to the precipitation of the secondary (impurity) phase YbOF. Since the presence of metal over-growth of ytterbium is impossible because it is far too reactive. Furthermore, the acid cleaning does not remove the feature, and YbOF is known to be insoluble in acid.

The secondary crystallization of ROF(R = La, Yb) in the case of $RCrO_3$(R = La, Yb) crystals takes place beside the growth of the latter from the flux system PbO–PbF_2–B_2O_3. However, all the evidence favours the crystallization of ROF nearly at the end of the growth of $RCrO_3$ crystals. The results are further supported [6–8] where it is suggested that the formation of ROF (R = Er, Ho, Dy) phases in the case of rare-earth orthoferrite, $RFeO_3$ (R = Er, Ho, Dy) crystals takes place.

4. Conclusions

1. Flux grown $RCrO_3$(R = La, Yb) crystals show cracks which become preferential places for the accumulation of undissolved flux which may contain lead as well as lanthanum and chromium.
2. The cracks are probably produced by the contracting of $RCrO_3$ crystals on cooling.
3. Using the PbO–B_2O_3–PbF_2 flux system for the growth of $RCrO_3$(R = La, Yb) crystals results in the precipitation of lead-associated materials, for example,

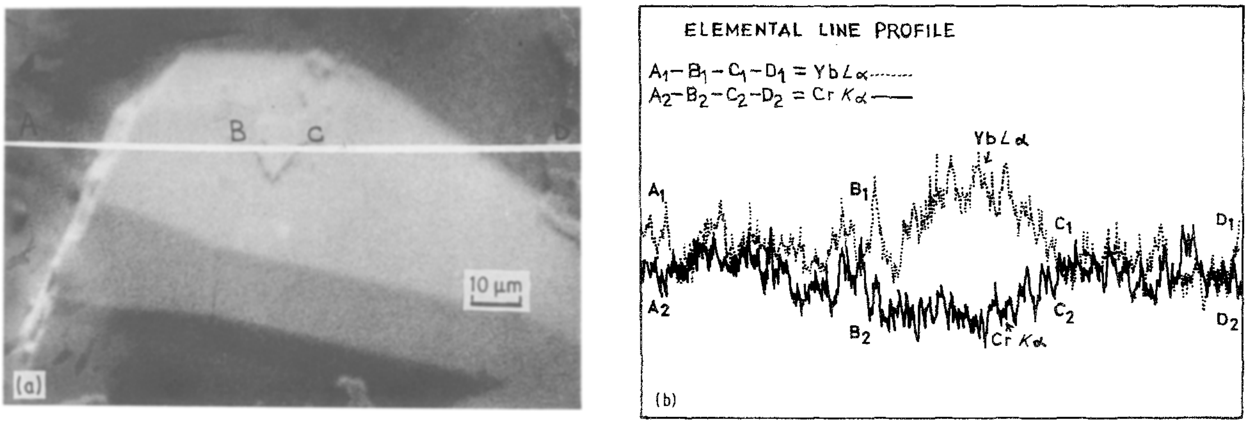

Figure 8 (a) SEM of $YbCrO_3$ surface showing a triangular structure (B–C). The line A–B–C–D is the route of the elemental scan. (b) Elemental line profile displaying the detection of Yb$L\alpha$ and Cr$K\alpha$. There is a loss of Cr$K\alpha$ (B_2–C_2) radiation and a rise in Yb$L\alpha$ (B_1–C_1) confirming the presence of ytterbium.

Pb_2CrO_5, incompletely dissolved flux (Pb_2OF_2) or lead combined with chromium, oxide and a rare-earth element $R(R = La, Yb)$.

4. Entry of lead as a major constituent wherever and whenever it takes place, is at the expense of $R(R = La, Yb)$ and chromium in most of the cases of the $RCrO_3(R = La, Yb)$.

5. Other impurity phases, LaOF and YbOF, also get precipitated in the case of $LaCrO_3$ and $YbCrO_3$ crystals, respectively.

6. Deposition of impurity phases in the shape of typical structures in case of $RCrO_3(R = La, Yb)$ crystals, however, takes place apparently after the crystals cease to grow, as there is no evidence of any modification of growth fronts.

Acknowledgements

The authors are grateful to Dr G. Garton, Head of the Crystal Growth Group, University of Oxford, for his great interest and encouragement in the collaborative research programme between the Physics Department, University of Jammu and his laboratory. One of the authors (AKR) is thankful to the University Authorities for the award of University Fellowship. The help rendered by Mr V. G. Shah and the authorities of PRL, Ahmedabad during SEM and EDAX work are gratefully acknowledged.

References

1. J. P. REMEIKA, *J. Amer. Chem. Soc.* **78** (1956) 4259.
2. B. M. WANKLYN Jr. *Cryst. Growth* **5** (1969) 323.
3. P. N. KOTRU, S. C. GOSWAMI and B. M. WANKLYN, *J. Mater. Sci.* **18** (1983) 3729.
4. P. N. KOTRU, S. K. KACHROO, A. K. RAZDAN, K. K. RAINA and B. M. WANKLYN, *Bull. Elect. Micro. Soc. India* **7** (1983) 113.
5. P. N. KOTRU, S. K. KACHROO and B. M. WANKLYN, *J. Mater. Sci. Lett.* **4** (1985) 1273.
6. *Idem, J. Mater. Sci.* **21** (1986) 1609.
7. *Idem, ibid.* **21** (1986) 3625.
8. P. N. KOTRU, S. K. KACHROO, B. M. WANKLYN and B. E. WATTS, *ibid.* **22** (1987) 4484.
9. P. N. KOTRU, A. JAIN, A. K. RAZDAN and B. M. WANKLYN, *J. Mater. Sci.* (in press).
10. B. M. WANKLYN, F. R. WONDRE, B. J. GARRARD and S. H. SMITH, *ibid.* **13** (1978) 89.
11. T. D. MCKILNEY, K. F. J. HEINRICH and D. B. WITTRY, (eds) "The Electron Microprobe Wiley", New York (1966).

Received 17 August
and accepted 9 September 1988